Extensional flow-based microfluidic device: deformability assessment of red blood cells in contact with tumor cells

Vera Faustino[1], Diana Pinho[1], Tomoko Yaginuma[1], Ricardo C. Calhelha[1, 2], Isabel C.F.R. Ferreira[1, 2] & Rui Lima[1, 3]

[1] Polytechnic Institute of Bragança, IPB, C. Sta. Apolónia, 5301-857 Bragança, Portugal.
[2] CIMO, C. Sta. Apolónia, 5301-857 Bragança, Portugal.
[3] CEFT, Faculdade de Engenharia da Universidade do Porto (FEUP), R. Dr. Roberto Frias, 4200-465 Porto, Portugal.
* Correspondence and requests for materials should be addressed to R. Lima (ruimec@ipb.pt)

Abstract Red blood cell (RBC) deformability has become one of the important factors to assess blood and cardiovascular diseases. The interest on blood studies have promoted a development of various microfluidic devices that treat and analyse blood cells. Recent years, besides the RBC deformability assessment, these devices are often applied to cancer cell detection and isolation from the whole blood. The devices for cancer cell isolation rely mainly on size and deformability of the cells. However, the examination of deformability of the RBCs mixed with cancer cells is lacking. This study aims at determining the deformation index (DI) of the RBCs in contact with cancer cells using a hyperbolic microchannel which generates a strong extensional flow. The DIs of human healthy RBCs and human RBCs in contact with a tumor cell line (HCT-15, colon carcinoma) were compared by analyzing the flowing RBCs images captured by a high speed camera. The results reveal that the RBCs that were in contact with HCT-15 cells have lower deformability than the normal RBCs.

Keywords: Biomicrofluidics, Microfluidic devices, Blood on chips, Red blood cells, Cell deformability, Deformation index

Introduction

Red blood cells (RBCs) deformability is the ability of RBCs to deform when submitted to certain flow conditions. The major determinants of the deformability include geometry and size of the microvessels, flow rate, mechanical properties of the cell membrane and its cytoskeleton and intracellular viscosity. For example, the RBCs elongate significantly when they pass through microchannels with dimensions smaller than the diameter of the RBCs at rest [1-5]. Decreased RBC deformability is a threat to human health, since it causes a clog in the small capillaries. Therefore, RBC deformability evaluation has become a research interest in a range of research fields.

In biomechanical and microfluidics studies, the clinical significance of RBC deformability has been promoting the development of methods for measuring this phenomenon. Some examples are the RBC filtration [6], laser diffraction ellipsometry [7], rheoscopy [8], micropipette aspiration [9] and cytometry [10]. Recently, by using a soft lithography technique it is possible to fabricate transparent microchannels to investigate the motion and dynamical deformation of cells [3, 11-17].

The microfluidic device technologies have been recognized as a promising, high-throughput method for diseased cell studies [18]. Besides the assessment of blood cells themselves, another application is associated with cancer cell detection in a blood flow. One of the focussed research interests is a circulating tumor cell (CTC) detection and isolation from the whole blood [19-23]. Largely, there are two major device designing strategies: one is to create arrays of narrow gaps within

a larger microchannel and catch the cancerous cells in these gaps leaving other blood cells passing through the gaps [19,20], and the other is to sort the heterogeneous cells such as a mixture of RBCs, white blood cells and cancerous cells by using an inertial migration force under the flow in a microchannel where the cells tend to migrate toward different lateral equilibrium positions and eventually are sorted into separate regions of the microchannel [21-23]. Importantly, for both strategies a key issue is the size and deformability of the cells. The former method requires a careful design for the width of the gaps, otherwise the deformable cells, including both RBCs and cancer cells would not be able to be sorted accurately. For the latter case, the size and deformability of the cells greatly influence the flow behaviour and consequently lateral equilibrium positions might be altered. For instance, it is known that the highly deformable cells migrate towards the center of the microchannel whereas the rigid cells are pushed away from the center. Without a good knowledge of mechanical properties of healthy and diseased cells, a high efficiency of cell sorting will not be achieved. As mentioned above, there are a number of studies for development of microfluidic devices for cancer cell separation from a mixture of blood cells and cancerous cells but to our knowledge no insightful investigation has been done for characterizing deformability, by using DI, of the RBCs in contact with cancer cells. As RBC deformability is one of the most important properties for designing microfluidic devices for sorting heterogeneous cells, there is a need to examine the deformability of RBCs which were in contact with cancer cells.

In this paper, we examine deformability of human RBCs mixed with HCT-15 (colon carcinoma) using the microchannel having a hyperbolic shape in which the fluid experiences a strong extensional flow with a nearly constant strain rate at the centerline of the microchannel. The deformability is characterized by deformation index (DI) measuring the major and minor axis lengths of the RBCs flowing near the centreline of the microchannel. The influence of the time duration that the RBCs were in contact with the cancer cells is also examined.

Materials and Methods

Working fluids and microchannel geometry

The working fluid used in this study was Hank's Balanced Salt Solution (HBSS) containing 2% Hct of human RBCs and the preparation was done as follows. The blood was collected from a healthy adult volunteer, and ethylenediaminetetraacetic acid (EDTA) was added to prevent coagulation. The RBCs were separated from the plasma and buffy coat by centrifugation (1000 rpm for 10 min). The RBCs were then washed and centrifuged with HBSS twice. Washed RBCs were diluted with HBSS to make several samples with hematocrit levels of ~2% by volume. All blood samples were stored hermetically at 4ºC until the labelling.

A human tumor cell line HCT-15 (colon carcinoma) was used to mix with RBCs. Cells were routinely maintained as adherent cell cultures in culture medium so that RPMI 1640 was supplemented with fetal bovine serum (10% FBS), streptomycin/penicillin antibiotic, 2 mM glutamine, and essential amino acids, at the temperature of 37ºC, in a humidified air incubator containing 5% of CO_2. Each cell line was plated at an appropriate density (2×10^5 cells/well HCT-15) in 6-well plates and mixed with 1 ml of RBCs (2% Hct) (c.f. Fig. 1). One sample of RBCs mixed with tumor cell line was taken after 24h of incubation and another one after 48h. Note that for these samples, only RBCs were taken by a micropipette and the tumor cells were not used for the flow experiments.

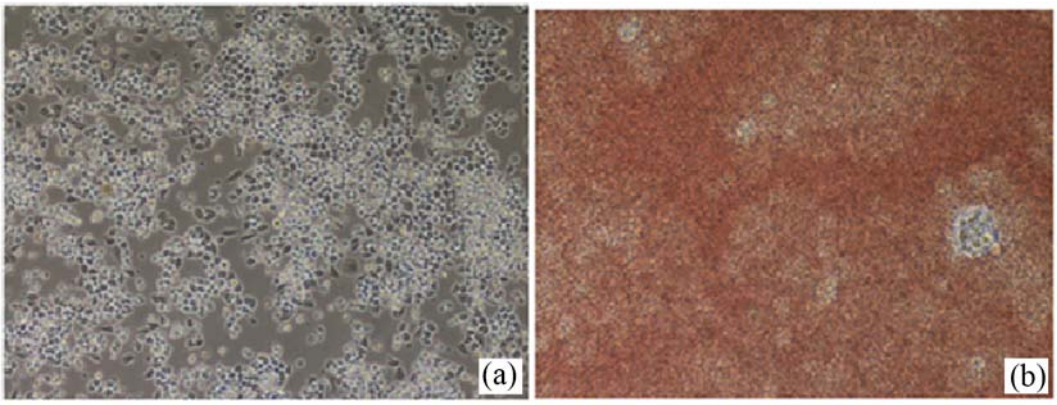

Figure 1. Images of cell culturing after 24h of incubation. (a) HCT-15 cell line only, (b) HCT-15 cell line mixed with RBCs. HCT-15 cells are attached on the bottom of the dish so that the suspended RBCs (red color cells) are more visible.

In order to avoid the possibility of the influence other than tumor cells' contact on RBCs, the samples of RBCs only with HBSS and RBCs only with the medium were also prepared. All the samples prepared are summarized in Table 1.

The hyperbolic microchannel geometry and the regions for DI measurement are shown in Fig. 2.

Table 1. Sample preparation

Case	Cell sample	Incubation time (h)	Temperature (ºC)	CO_2 (%)
1	RBCs with HBSS	-	Room temperature	-
2	RBCs with medium	24h	37ºC	5%
3	RBCs with medium	48h	37ºC	5%
4	RBCs with HCT-15 cell line	24h	37ºC	5%
5	RBCs with HCT-15 cell line	48h	37ºC	5%

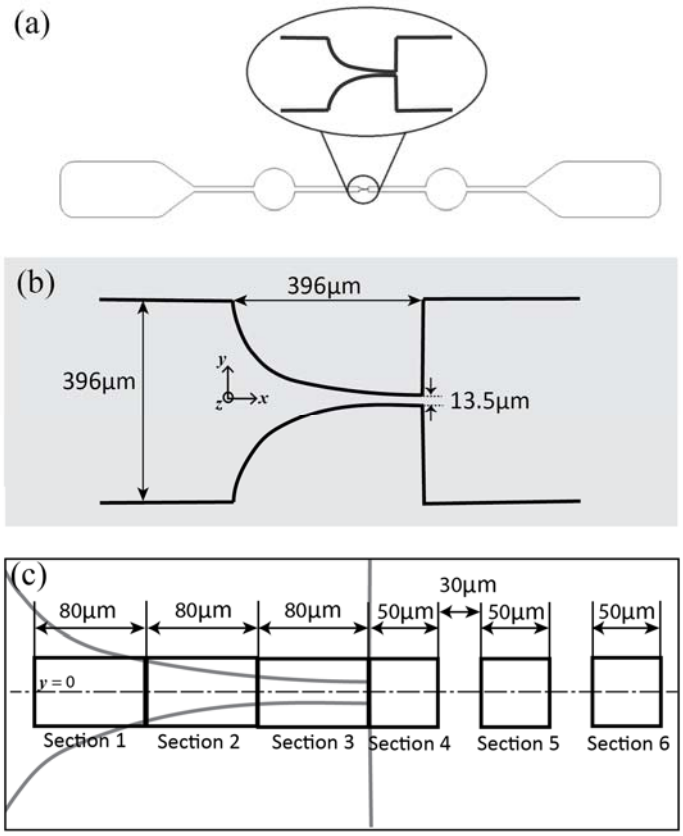

Figure 2. (a) Illustration of the entire microchannel view, (b) schematic diagram and geometries of the microchannel focused on the hyperbolic contraction part, (c) deformation measurement sections with corresponding lengths in microns.

Experimental set-up

Fig. 3 shows a schematic of the experimental set-up. The confocal system of an inverted microscope (Diaphot 300, Nikon) combined with a high-speed camera (FASTCAM SA3, Photron) was used in the present study. A polydimethylsiloxane (PDMS) microchannel having a hyperbolic shape was manufactured by using a soft-lithography technique. As described in Fig. 2, the dimension of the microchannel is 396µm (w) × 396 µm (l) ×14 µm (h) where w, l and h refer to the width of the inlet microchannel, the length of the hyperbolic contraction region and the depth of the microchannel. The PDMS microchannel was placed on the stage of the microscope where the flow rate Q of the working fluids was kept constant (0.5µl/min) by means of a syringe pump (PHD ULTRA) with a 1mL syringe (TERUMO ® SYRING). The flowing RBCs were recorded by the high speed camera at a frame rate of 7500 frames/s and then the digital images were analysed with the assistance of an image handling software.

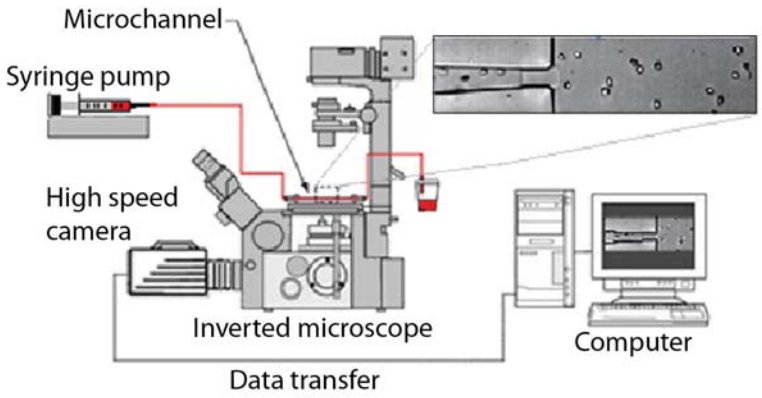

Figure 3. Experimental set-up.

Image Analysis

Fig. 4 shows the steps of image processing with the corresponding actual images in each step. Briefly, the original video data was converted to a stack of JPEG images (Fig. 4a). Then by averaging each pixel over the sequence of original images (stack), a background image was created (Fig. 4b). The background image contains the objects that are static in all the images such as microchannel walls, dusts and so on. The next step is to subtract the background image from the stack images. This process eliminates all the static objects from the original images and leaves only RBCs visible (Fig. 4c). The images were then filtered by replacing each pixel with the median of the neighbouring pixel values with a mask size of 3×3 pixels, in order to reduce the artifacts and enhance the image quality. The brightness and contrast of the resulted images were also manually adjusted. Finally, the grey scale images were converted to binary images adjusting the threshold level (Fig. 4d). Well-known Otsu threshold method was used in this case [24]. The resulted images contain RBCs as black edged ellipsoidal objects against a white background. After this segmentation process, the flowing RBCs were measured frame by frame automatically by using *Analyze Particles* function in ImageJ [25]. This function counts and measures the objects in binary images, by detecting the edge of the objects and outlining them (Fig. 4e). Various parameters for measurement such as area and circularity of the cells were appropriately pre-set so that the values outside the range specified are ignored. For instance, we set the range of area as 17-150 μm^2 such that the objects smaller than 17 μm^2 and larger than 150 μm^2 are eliminated from the results table. Likewise, the circularity range was set to be 0.5-1.0. Here the circularity is defined as $4\pi \times (\text{area}) / (\text{perimeter})^2$. This way, most of the apparent deviant objects (eg. out-of-focus cells, aggregated cells, etc.) were ignored for measurements.

The major output results of this measurement are the major (X) and minor (Y) axis lengths of the ellipse that can be best fitted to the RBCs. The *x*-*y* coordinates of the measured cells' centroids were also recorded so that the position of the cells can be identified. Using this set of data, the DIs of all the measured cells were calculated by using the formula of (X-Y)/(X+Y). The DI value is between 0 and 1, in that 0 means a perfect circle and the higher value means more deformed shape. In this study, we calculated DIs for all the RBCs located in the sections of interest (Fig. 2c) and averaged the values for each section.

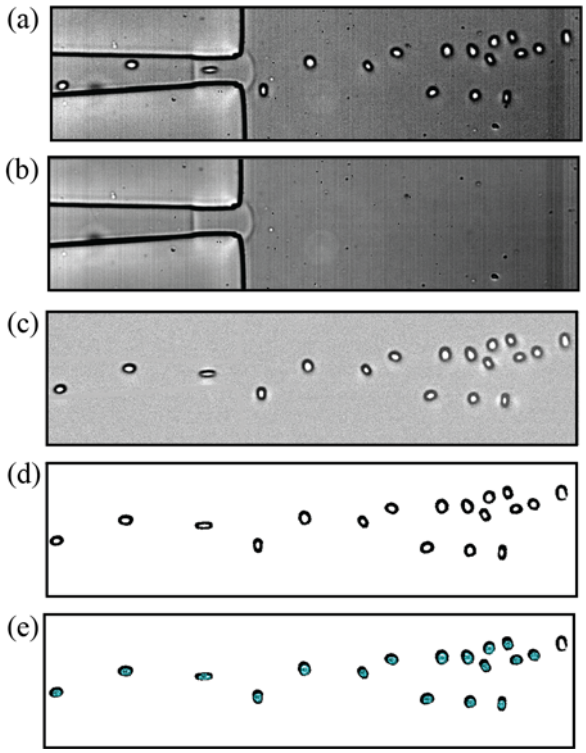

Figure 4. Steps of image analysis. (a) original image, (b) created background image, (c) subtracted image where only RBCs are visible, (d) binarized image by thresholding, (e) RBCs outlined by ImageJ, Analyze Particles function.

Results and Discussion

Fig. 5 shows the comparison of DIs among the three control cases (c.f. RBCs with HBSS, RBCs with medium for 24h and RBCs with medium for 48h). For each case, the mean DI values for six pre-defined regions in the microchannel were shown (c.f. Fig.2c).

The DI values and tendency of the transition are very similar in all the cases. In the contraction regions (Sections 1, 2 and 3), the DI values are high under the strong extensional flow, and tend to increase as the cells proceed to the exit of the contraction part. In Section 3, in all the cases the DI reaches the maximum values. Then the DI drops dramatically in the release region (Section 4) and stay with the constant value in the consequent regions (Sections 5 and 6). These tendencies consolidate that through the microchannel with a hyperbolic shaped contraction the RBCs experience strong extensional force and deform significantly. It is worth noting that the DI differences between RBCs with HBSS and medium are not seen. Moreover, the RBC deformability does not show significant difference in terms of time duration for the cases of RBCs with medium for 24h and 48h. It is important to examine these control cases so that the other cases, that are RBCs mixed with tumor cells, can prove that the influence on RBCs deformability is extremely limited to the contact of tumor cells.

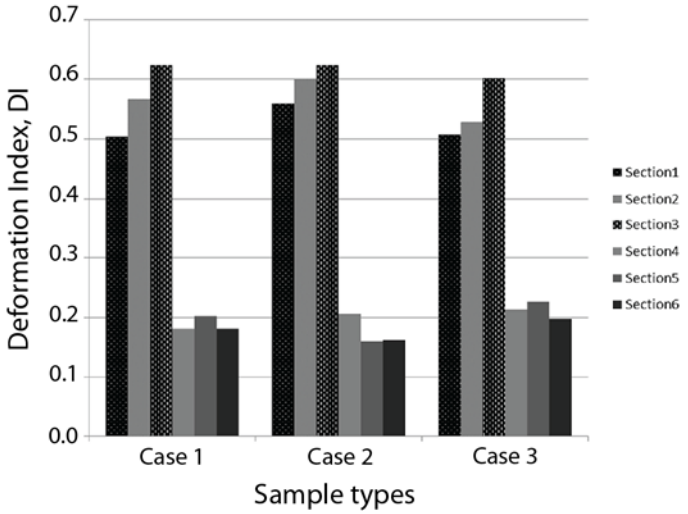

Figure 5. RBC deformation index for Case 1, 2 and 3. Note that Case 1 is RBCs with HBSS, Case 2 is RBCs with medium for 24h, and Case 3 is RBCs with medium for 48h.

Fig. 6 compares RBC deformation between RBCs with medium and RBCs mixed with HCT-15 as a function of time duration: 24h and 48h. It reveals that the RBCs mixed with HCT-15 show extremely low DI compared with the RBCs with medium in the contraction regions. This implies the RBCs in contact with HCT-15 became more rigid than healthy RBCs. It is also possible to say that an increase of rigidity occurred within 24h after a mixture with HCT-15 and this status did not change with time (see Fig. 6b for 48h case). Although there is a tendency that the DI values increase towards the exit of the contraction part and then drops after the release, the maximum value of RBCs in contact with HCT-15 is almost half of that of the RBCs with medium. The DI values for the Sections 4, 5 and 6 do not show significant differences among the cases shown in Fig. 6.

It is reported that an increase of RBC rigidity is caused by lowering pH, elevating temperature, increasing extracellular glucose concentration, or making the suspending medium hypo- or hypertonic [26-28]. Moreover, there are studies that cancer cells are more acidic than normal cells and generate acidic or low pH microenvironment which is ideal for invasion and metastasis [29,30]. Considering the phenomena of all the above, the observed RBCs rigidity in the current study was possibly due to the influence of tumor cells' acidity or the acidic environment generated by the tumor cells. In most studies on cancer cell isolation from blood cells, microchannel devices are designed based on the hypothesis that the healthy RBCs are highly deformable cells. However, our results have shown that the increase of RBC rigidity could occur when RBCs were mixed with cancer cells in a culturing stage and its increase degree was not ignorable. In order to achieve high throughput of cancer cell isolation, it is necessary to take into account that the possible alteration of RBC deformability can happen and this property change could directly influence flow behaviour and migration tendency which are the key issues in designing microfluidic devices. Further investigation on RBC deformability and cell sorting based on the current study will be conducted in the near future and will be shared in due course.

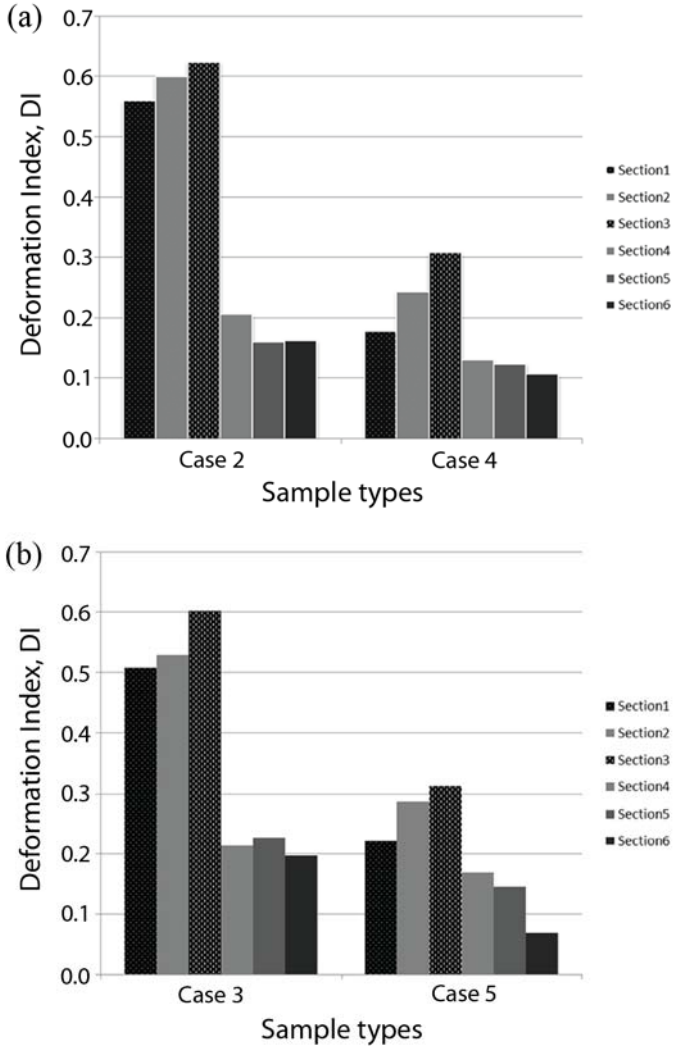

Figure 6. (a) RBC deformation index for Case 2 and 4, (b) RBC deformation for Case 3 and 5. Note that Case 2 is RBCs with medium for 24h, Case 4 is RBCs with HCT-15 for 24h, Case 3 is RBCs with medium for 48h, and Case 5 is RBCs with HCT-15 for 48h.

Acknowledgment The authors acknowledge the financial support provided by: Student Mobility Placements with the program Lifelong Learning (Erasmus Program), 2007 Global COE Program "Global Nano-Biomedical Engineering Education and Research Network", Japan. Grant-in-Aid for Science and Technology (PTDC/SAU-BEB/105650/2008, PTDC/EME-MFE/099109/2008 and PTDC/SAU-ENB/116929/2010) from the Science and Technology Foundation (FCT) and COMPETE, Portugal. The authors are also very grateful to Professor Mónica S.N. Oliveira (Strathclyde University), Professor Geyong M. Kim (University of Navarra) and Professor Sergio Arana (University of Navarra) for their discussion and suggestions to this research work.

References

[1] Caro, C., Pedley, T., Schroter, R., & Seed, W. *The Mechanics of the Circulation*. Oxford University Press, (1978).

[2] Skalak, R., & Branemark, P-I. Deformation of red blood cells in capillaries. *Science* **164**, 717-719

(1969).

[3] Abkarian, M., *et al*. Cellular-scale hydrodynamics. *Biomed Mater* **3**, 034011 (2008).

[4] Hardeman, M.R., & Ince, C. Clinical potential of *in vitro* measured red cell deformability, a myth? *Clin Hemorheol Microcirc* **21**, 277-284 (1999).

[5] Cho, Y.I., Mooney, M.P., & Cho, D.J. Hemorheological disorders in diabetes mellitus. *J Diabetes Sci Technol* **2**, 1130-1138 (2008).

[6] Gueguen, M., *et al*. Filtration pressure and red blood cell deformability: evaluation of a new device: erythrometre. Biorheology Suppl **1**, 261-265 (1984).

[7] Shin, S., Ku, Y., Park, M.S., & Suh, J.S. Measurement of red cell deformability and whole blood viscosity using laser-diffraction slit rheometer. *Korea-Australia Rheol J* **16**, 85-90 (2004).

[8] Dobbe, J.G.G., *et al*. Analyzing red blood cell-deformability distributions. *Blood Cells Mol Dis* **28**, 373-384 (2002).

[9] Mokken, F.C., Kedaria, M., Henny, C.P., Hardeman, M.R., & Gelb, A.W. The clinical importance of erythtrocyte deformability, a hemorrheological parameter. *Ann Hematol* **64**, 113-122 (1992).

[10] Bow, H., *et al*. A microfabricated deformability-based flow cytometer with application to malaria. *Lab Chip* **11**, 1065-1073 (2011).

[11] Lima, R., *et al*. In vitro blood flow in a rectangular PDMS microchannel: experimental observations using a confocal micro-PIV system. *Biomed Microdevices* **10**, 153-167 (2008).

[12] Fujiwara, H., *et al*. Red blood cell motions in a high hematocrit blood flowing through a stenosed micro-channel. *J Biomech* **42**, 838-843 (2009).

[13] Lima, R., *et al*. Axisymmetric PDMS microchannels for in vitro haemodynamics studies. *Biofabrication* **1**, 035005 (2009).

[14] Lee, S.S., Yim, Y., Ahn, K.H., & Lee, S.J. Extensional flow-based assessment of red blood cell deformability using hyperbolic converging microchannel. *Biomed Microdevices* **11**, 1021-1027 (2009).

[15] Zhao, R., *et al*. Microscopic investigation of erythrocyte deformation dynamics. *Biorheology*, **43**, 747-765 (2006).

[16] Yaginuma, T., Oliveira, M.S.N., Lima, R., Ishikawa, T., & Yamaguchi, T. Human red blood cell behavior under homogeneous extensional flow in a hyperbolic-shaped microchannel, *Biomicrofluidics* **7**, 054110 (2013).

[17] Pinho, D., Yaginuma, T., & Lima, R. A microfluidic device for partial cell separation and deformability assessment. *BioChip J* **7**, 367-374 (2013).

[18] Hou, H.W., *et al*. Microfluidics for applications in cell mechanics and mechanobiology. *Cel Mol Bioeng* **4**, 591–602, (2011).

[19] Tan, S.J., Yobas, L., Lee, G.Y., Ong, C.N., & Lim, C.T. Microdevice for the isolation and enumeration of cancer cells from blood. *Biomed Microdevices* **11**, 883-892 (2009).

[20] Mohamed, H., Murray, M., Turner, J.N., & Caggana, M. Isolation of tumor cells using size and deformation. *J Chromatogr A* **1216**, 8289-8295 (2009).

[21] Hur, S.C., Henderson-MacLennan, N.K., McCabe, E.R., & Di Carlo, D. Deformability-based cell classification and enrichment using inertial microfluidics. *Lab Chip* **11**, 912-920 (2011).

[22] Tanaka, T., *et al*. Separation of cancer cells from a red blood cell suspension using inertial force. *Lab Chip* **12**, 4336-4343 (2012).

[23] Lee MG, Shin JH, Bae CY, Choi S, & Park JK. Label-free cancer cell separation from human whole blood using inertial microfluidics at low shear stress. *Anal Chem* **85**, 6213-6218 (2013).

[24] Otsu, N. A threshold selection method from gray-level histograms. *IEEE Trans Sys Man Cyber* **9**, 62-66 (1979).

[25] Abramoff, M.D., Magalhaes, P.J., & Ram, S.J. Image Processing with ImageJ. *Biophotonics Int* **11**, 36-42 (2004).

[26] Jain, R.K. Determinants of tumor blood flow: a review. *Cancer Res* **48**, 2641-2658 (1988).

[27] Sevick EM, & Jain RK. Effect of red blood cell rigidity on tumor blood flow: increase in viscous resistance during hyperglycemia. *Cancer Res* **51**, 2727-30 (1991).

[28] Kuzman, D., *et al*. Effect of pH on red blood cell deformability. Pflugers Arch **440**, R193-194 (2000).

[29] Griffiths, J.R. Are cancer cells acidic? *Br J Cancer* **64**, 425-427 (1991).

[30] Estrella, V., *et al*. Acidity generated by the tumor microenvironment drives local invasion. *Cancer Res* **73**, 1524-1535 (2013).